



ZFP36 ring finger protein like 1 significantly suppresses human coronavirus OC43 replication

Tooba Momin¹, Andrew Villasenor¹, Amit Singh¹, Mahmoud Darweesh^{2,3}, Aditi Singh¹ and Mrigendra Rajput¹

¹ Department of Biology, University of Dayton, Dayton, OH, United States of America

² Department of Medical Biochemistry and Microbiology, Uppsala University, Uppsala, Uppsala, Sweden

³ Department of Microbiology and Immunology, Faculty of Pharmacy, Al-Azhr University, Assiut, Egypt

ABSTRACT

CCCH-type zinc finger proteins (ZFP) are small cellular proteins that are structurally maintained by zinc ions. Zinc ions coordinate the protein structure in a tetrahedral geometry by binding to cystine-cystine or cysteines-histidine amino acids. ZFP's unique structure enables it to interact with a wide variety of molecules including RNA; thus, ZFP modulates several cellular processes including the host immune response and virus replication. CCCH-type ZFPs have shown their antiviral efficacy against several DNA and RNA viruses. However, their role in the human coronavirus is little explored. We hypothesized that ZFP36L1 also suppresses the human coronavirus. To test our hypothesis, we used OC43 human coronavirus (HCoV) strain in our study. We overexpressed and knockdown ZFP36L1 in HCT-8 cells using lentivirus transduction. Wild type, ZFP36L1 overexpressed, and ZFP36L1 knockdown cells were each infected with HCoV-OC43, and the virus titer in each cell line was measured over 96 hours post-infection (p.i.). Our results show that HCoV-OC43 replication was significantly reduced with ZFP36L1 overexpression while ZFP36L1 knockdown significantly enhanced virus replication. ZFP36L1 knockdown HCT-8 cells started producing infectious virus at 48 hours p.i. which was an earlier timepoint as compared to wild -type and ZFP36L1 overexpressed cells. Wild-type and ZFP36L1 overexpressed HCT-8 cells started producing infectious virus at 72 hours p.i. Overall, the current study showed that overexpression of ZFP36L1 suppressed human coronavirus (OC43) production.

Subjects Agricultural Science, Microbiology, Molecular Biology, Veterinary Medicine, Virology

Keywords CCCH type Zinc finger protein, ZFP36L1, RNA binding protein, Human coronavirus OC43

INTRODUCTION

CCCH-type zinc finger proteins (ZFPs) are small cellular proteins that are structurally maintained by zinc ions. Zinc ions coordinate the protein structure in a tetrahedral geometry (Abbehausen, 2019; Hajikhezri et al., 2020). There are over 40 different types of ZFPs that have been annotated so far (Hajikhezri et al., 2020). ZFP's unique structure enables it to interact with a wide variety of molecules such as DNA, RNA, PAR (poly-ADP-ribose), and cellular proteins and thus modulate several cellular processes including host

Submitted 16 August 2022
Accepted 3 January 2023
Published 20 February 2023

Corresponding author
Mrigendra Rajput,
mrjput1@udayton.edu

Academic editor
Mahendra Tomar

Additional Information and
Declarations can be found on
page 10

DOI 10.7717/peerj.14776

© Copyright
2023 Momin et al.

Distributed under
Creative Commons CC-BY 4.0

OPEN ACCESS

immune response and virus replication (Müller *et al.*, 2007; Cassandri *et al.*, 2017; Takata *et al.*, 2017; Tang, Wang & Gao, 2017; Meagher *et al.*, 2019; Lal, Ullah & Syed, 2020). Among various ZFPs, the CCCH-type ZFP family contains zinc ions that coordinate protein structure by binding to cystine-cystine or cysteines-histidine amino acids (Abbehausen, 2019; Hajikhezri *et al.*, 2020). The CCCH-type ZFP family has also been characterized for its antiviral (Hajikhezri *et al.*, 2020; Tang, Wang & Gao, 2017; Zhang *et al.*, 2020; Guo *et al.*, 2004; Zhao *et al.*, 2019; Gao, Guo & Goff, 2002; Zhu *et al.*, 2020; Musah, 2004; Chen, Jeng & Lai, 2017; Scozzafava *et al.*, 2003; Schito *et al.*, 2006; Angiolilli *et al.*, 2021) and immune modulator activity (Wang *et al.*, 2015; Tu *et al.*, 2019; Haneklaus *et al.*, 2017; Lv *et al.*, 2021; Matsushita *et al.*, 2009; Wawro, Kochan & Kasza, 2016; Uehata & Akira, 2013; Chen *et al.*, 2018; Mino *et al.*, 2015; Fu & Blackshear, 2017; Stumpo, Lai & Blackshear, 2010; Shrestha, Pun & Park, 2018; Kontoyiannis, 2018).

CCCH-type ZFPs show their antiviral efficacy against several RNA viruses including Influenza A virus (Tang, Wang & Gao, 2017), retrovirus (Gao, Guo & Goff, 2002; Zhu *et al.*, 2011; Zhu *et al.*, 2017) filoviruses (Müller *et al.*, 2007), and alphavirus such as Sindbis virus, Semliki Forest virus, Ross River virus, and Venezuelan equine encephalitis virus (Bick *et al.*, 2003). However, CCCH-type ZFP's role on the human coronavirus is little explored. The current study is designed to evaluate the effect of ZFP36L1, a CCCH-type ZFP, on human coronavirus (HCoV)-OC43 replication.

MATERIALS & METHODS

Cells, virus strains and virus propagation

HCT-8 cells (ATCC, Manassas, VA, USA) were cultured in Roswell Park Memorial Institute (RPMI) 1640 Medium (Gibco BRL, Grand Island, NY, USA) and supplemented with 10% heat-inactivated fetal bovine serum (FBS), (ATCC, Manassas, VA, USA), and antibiotic-antimycotic: penicillin 100 units/ml, streptomycin 0.10 mg/ml and amphotericin B 0.25 µg/ml (Sigma-Aldrich, St. Louis, MO, USA). During virus culture, HCT-8 cells were adapted to 1% FBS. HCT-8 cells cultured with RPMI 1640 medium supplemented with 1% FBS were used to grow and subsequently titrate the OC43 human coronavirus (HCoV) stain (ATCC, Manassas, VA, USA).

Overexpression and knockdown of ZFP36L1

HCT-8 cells were stably overexpressed for ZFP36L1 (NCBI reference sequence: [NM_001244701.1](#)) with a green fluorescent protein (GFP) marker using a lentivirus vector. The ZFP36L1 gene containing both tandem zinc finger domains (TZFD) such as TZFD1 and TZFD2 were cloned in a pLV-eGFP plasmid with the help of Vector Builder Inc, IL. To make the lentivirus, pLV-eGFP plasmids containing our gene of interest were co-transfected with VSV-G and packaging plasmids encoding Gag/Pol and Rev in HEK293T cells. After 48 h, the supernatant containing the lentivirus was collected and purified by centrifugation followed by filtration. Purified lentivirus was concentrated using a sucrose gradient ultracentrifugation and this concentrated, purified lentivirus was used in the study.

Similar to ZFP36L1 overexpression, HCT-8 cells were knockdown for ZFP36L1 using ZFP36L1 specific shRNA (GTAACAAGATGCTCAACTATA). The ZFP36L1 shRNA was stably expressed using a lentivirus by cloning it in a pLV-mCherry plasmid. Lentivirus for ZFP36L1-shRNA was prepared as per the above-mentioned method by co-transfection of pLV-mCherry containing ZFP36L1 shRNA with VSV-G and packaging plasmids in HEK293T cells.

The prepared lentiviruses were used to either overexpress or knock down ZFP36L1. Successful lentivirus transduction was measured through GFP or mCherry expression for ZFP36L1 overexpression (GFP) or ZFP36L1 knockdown (mCherry), respectively. Transduced HCT-8 cells were selected with an increased concentration of puromycin (2–3 $\mu\text{g/ml}$) over 7 days. Selected cells were further characterized for ZFP36L1 overexpression or knockdown using a western blot with ZFP36L1-specific antibodies.

Western blot analysis for ZFP36L1 expression

To confirm ZFP36L1 overexpression or ZFP36L1 knockdown; wild type, ZFP36L1 overexpressed and ZFP36L1 knockdown HCT-8 cells were individually seeded in T25 flasks. When cells reached 75–80% confluency, cells were lysed using a radioimmunoprecipitation assay buffer (RIPA buffer) (Cell Signaling Technology, Danvers, MA, USA) supplemented with protease-phosphatase inhibitor (Cell Signaling Technology, Danvers, MA, USA). Lysates were then centrifuged at $3,000 \times g$ for 15 min at 4°C . The supernatant was collected and the protein concentration in each supernatant was measured using the PierceTM BCA Protein Assay Kit (Thermo Fisher Scientific, Waltham, MA, USA). 40 μg cell lysates were separated through 12% resolving SDS PAGE gel. After separation, proteins were transferred onto a polyvinylidene difluoride (PVDF) membrane (Thermo Fisher Scientific, Waltham, MA, USA). The PVDF membrane was blocked with 5% skimmed milk (Sigma-Aldrich, St. Louis, MO, USA) in Tris-buffered saline (TBS) for 1 h at room temperature followed by incubation with anti-ZFP36L1 antibody (1:1000) (Thermo Fisher Scientific, Waltham, MA, USA) and anti- β actin antibody (1:4000) (Cell Signaling Technology, Danvers, MA, USA) overnight at 4°C . After overnight incubation, membranes were washed with tris-buffered saline +0.1% Tween 20 (TBST) and incubated with HRP conjugated secondary antibodies (1:2000) for 1 h at room temperature. After washing, membranes were developed using the Pierce ECL Western Blotting Substrate (Thermo Fisher Scientific, Waltham, MA, USA). Images of the western blot were taken by the Odyssey XF Imaging System (LI-COR Biosciences, Lincoln, NE). Band intensity for ZFP36L1 proteins was normalized with β -actin using ImageJ software ([Schneider, Rasband & Eliceiri, 2012](#)). A significant difference in ZFP36L1 expression in ZFP36L1 overexpressed and knockdown cells compared to wild-type cells was estimated using a paired *T*-test.

Determining ZFP36L1's effect on HCT-8 cells viability

The effect of ZFP36L1 overexpression and its knockdown on cell viability was measured by trypan blue exclusion assay ([Strober, 2015](#)). Wild type, ZFP36L1 overexpressed and ZFP36L1 knockdown cells were individually seeded in 6 well plates (1.5×10^6 cell/well) in triplicate. 96 h post-seeding, cells were washed with sterilized phosphate-buffered saline

(PBS) and detached with 0.25% trypsin-EDTA (ATCC, Manassas, VA, USA). Detached cells were washed with PBS by centrifugation at $500 \times g$ for 5 min at 4°C , and then cells were stained with 0.4% trypan blue for 3 min and examined for cell. Changes in cell viability following ZFP36L1 overexpression or its knockdown compared to wild-type cells was estimated by paired *t*-test.

Measuring the effect of ZFP36L1 expression on virus titration

Wild type, ZFP36L1 overexpressed and ZFP36L1 knockdown HCT-8 cells were infected with HCoV-OC43 with 0.1 multiple of infection (MOI) individually. The supernatant from these cells was collected at 24 h, 48 h, 72 h, and 96 h p.i. Collected cell supernatants were then centrifuged at $1,000 \times g$ at 4°C for 15 min to remove cell debris and stored at -80°C until used. Once samples from all time points were collected, the HCoV-OC43 virus titer was determined as per the aforementioned method (*Reed & Muench, 1938*). Changes in virus titer in ZFP36L1 overexpressed or ZFP36L1 knockdown cells were compared to wild-type cells and statistically analyzed by a paired *T*-test.

Measuring the effect of ZFP36L1 expression on HCoV-OC43 replication

To measure the effect of ZFP36L1 overexpression or ZFP36L1 knockdown on HCoV-OC43 replication, we infected ZFP36L1 overexpressed, ZFP36L1 knockdown or wild type HCT-8 cells with HCoV-OC43 (MOI: 0.1). Infected cells were collected at 72 and 96 h p.i. Viral RNA was isolated from infected cells using the QIAamp Viral RNA Mini kit (Qiagen, Valencia, CA, USA). The viral nucleocapsid was quantified using qPCR (Stratagene MX3000P Real-Time Thermocycler; Stratagene Inc., La Jolla, CA, USA) in $25 \mu\text{l}$ reaction using syber green dye. Primer sequence for nucleocapsid (F: 5'-: GCTGTT TWTGTTAAG TCYAAA GT-3', R: 5'- ATTCTGATAGAGAGTGCYTAT Y-3') were used (*Al-Khannaq et al., 2016*) with qPCR amplification cycle at $95^\circ\text{C}/2$ min, 40 cycles of ($95^\circ\text{C}/15$ and $60^\circ\text{C}/1$ min) followed by melting curve cycle at: $95^\circ\text{C}/15$ s, $60^\circ\text{C}/1$ min and $95^\circ\text{C}/15$ s. Fold change in HCoV nucleocapsid expression in each cell was estimated by paired -test.

Statistical analysis

The significant change in HCoV-OC43 titer and virus replication in wild-type, ZFP36L1 overexpressed, or ZFP36L1 knockdown cells was estimated using a paired *T*-test with 95% degree of freedom. Virus titer in wild-type, ZFP36L1 overexpression or ZFP36L1 knockdown cells was repeated at least three times with calculations for average, standard deviation, and standard error.

RESULTS

ZFP36L1 was overexpressed or knockdown in HCT-8 cells

A stable ZFP36L1 overexpression with an upstream GFP marker in HCT-8 cells was generated using a lentivirus system. GFP expression in HCT-8 cells was considered positive for ZFP36L1 overexpression (*Fig. 1B*), which was further confirmed by western blot (*Figs. 2 and 3*). Similarly, ZFP36L1 was knockdown using ZFP36L1-specific shRNA. The shRNA was located downstream to mCherry and expression of ZFP36L1-specific shRNA was

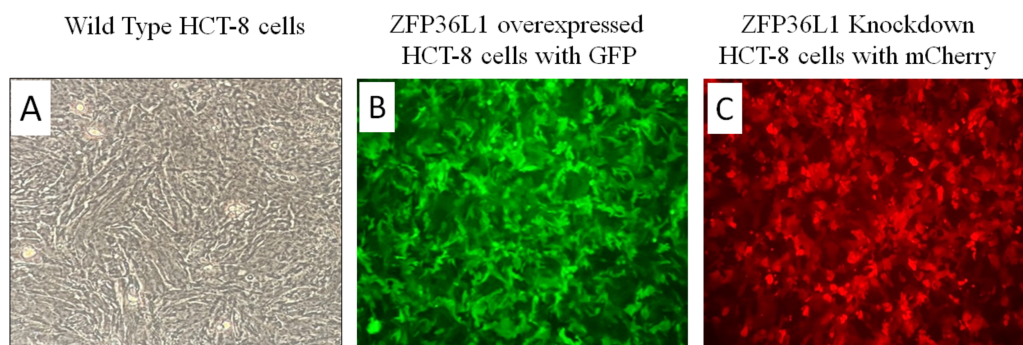


Figure 1 Overexpression and knockdown of ZFP36L1 in HCT-8 cells. Wild type HCT8 wells (A), ZFP36L1 overexpressed HCT-8 cells with GFP marker (B), and ZFP36L1 knockdown HCT-8 cells with mCherry marker (C). Overexpression and knockdown of ZFP36L1 were performed by lentivirus transduction.

Full-size DOI: 10.7717/peerj.14776/fig-1

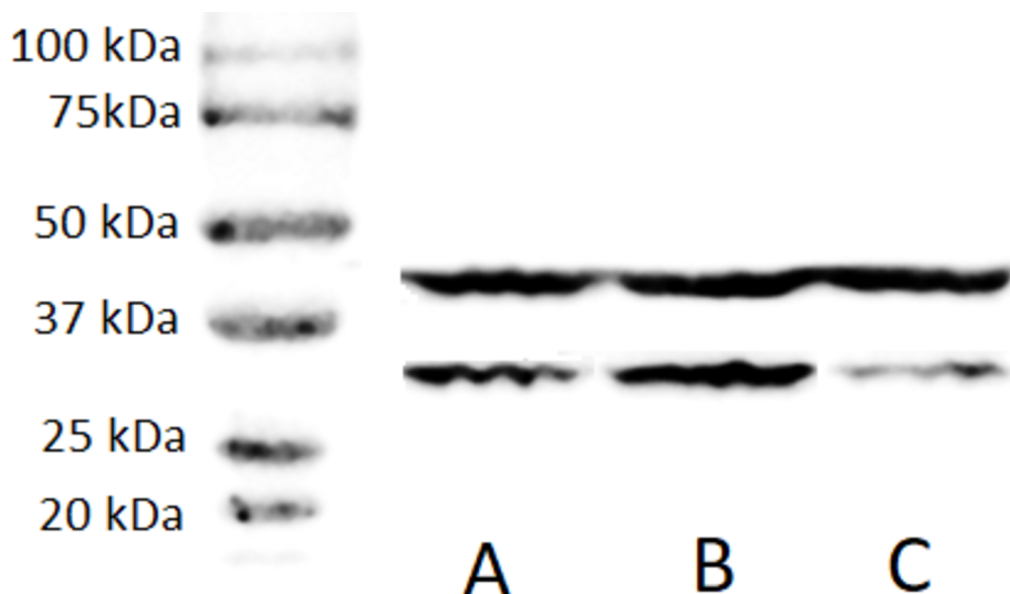


Figure 2 Western blot for confirming ZFP36L1 overexpression and knockdown in HCT-8 cells. Cell lysate for wild type HCT-8 cell (A), ZFP36L1 overexpressed (B) and ZFP36L1 knockdown (C) were separated with 12% resolving SDS PAGE gel and transferred to PVDF membrane. Proteins on the membrane were detected with an anti-ZFP36L1 antibody and anti- β actin antibody with HRP-conjugated secondary antibodies.

Full-size DOI: 10.7717/peerj.14776/fig-2

determined by mCherry expression (Fig. 1C) and ZFP36L1 knockdown was confirmed by western blot analysis (Figs. 2 and 3). Our results showed that lentivirus significantly overexpressed or knockdown ZFP36L1 in HCT-8 cells ($p < 0.05$) (Figs. 2 and 3).

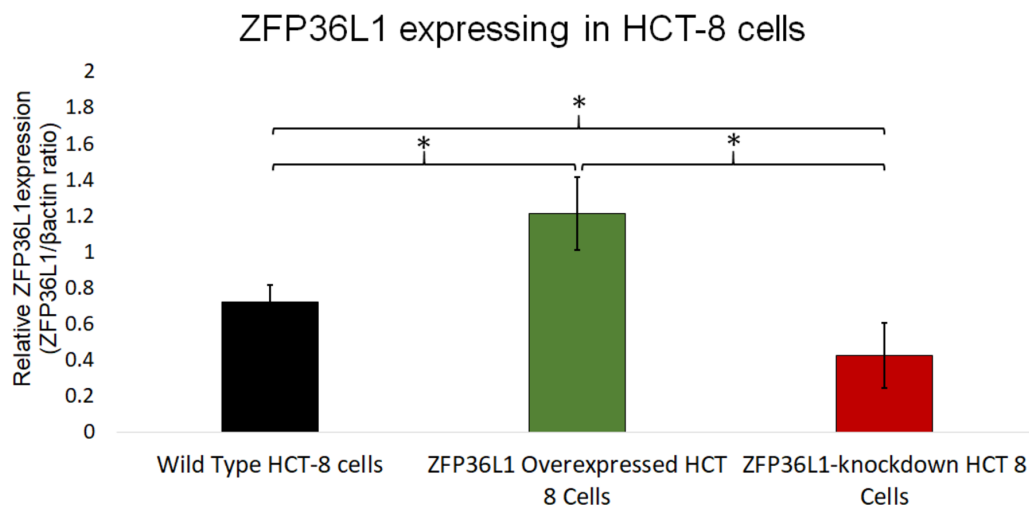


Figure 3 Relative quantification of ZFP36L1 expression in HCT-8 cell following its overexpression and knockdown. Cell lysate for wild-type HCT-8 cell, ZFP36L1 overexpressed and ZFP36L1 knockdown was analyzed for ZFP36L1 and β actin using western blot. Band intensity for ZFP36L1 proteins was normalized with β actin using ImageJ software. A significant difference in ZFP36L1 expression in ZFP36L1 overexpressed and knockdown cells compared to wild-type cells was estimated using a paired *T*-test. Asterisks show significant differences in ZFP36L1 expression.

Full-size DOI: [10.7717/peerj.14776/fig-3](https://doi.org/10.7717/peerj.14776/fig-3)

ZFP36L1 overexpressing or its knockdown did not affect HCT-8 cells' viability

The effect of ZFP36L1 overexpression or its knockdown was measured on HCT-8 cells' viability using trypan blue exclusion assay. The results showed that overexpression or knockdown of ZFP36L1 in HCT-8 cells did not affect its viability. Wild type, ZFP36L1 overexpressed and ZFP36L1 knockdown cells showed viability as $94.83 \pm 1.01\%$, $94.16 \pm 0.71\%$, and $95.83 \pm 0.43\%$ at 96 h post seeding, respectively. These values were non-significant different to each other ($p < 0.05$) (Fig. 4). Additionally, no apparent morphological changes were observed among these cells.

ZFP36L1 overexpression significantly suppressed, while ZFP36L1 knockdown significantly enhanced the HCoV-OC43 production

Wild type, ZFP36L1 overexpressed, and ZFP36L1 knockdown HCT-8 cells were infected individually with HCoV-OC43 with a MOI of 0.1. Cell supernatants were collected at 24 h, 48 h, 72 h, and 96 h p.i. and analyzed for virus titer.

The results showed that ZFP36L1 overexpression in HCT-8 cells significantly reduced virus titer ($p < 0.05$) (Fig. 5). Virus titer in ZFP36L1 overexpressed cells was 2.24 ± 1.28 log 10/ml and 4.32 ± 0.00 log 10/ml at 72 h and 96 h p.i. respectively. These titer values were significantly lower than virus titers in wild-type cells at same time points, such as 72 h p.i. (4.08 ± 0.11 log 10/ml) and 96 h p.i. (5.42 ± 0.10 log 10/ml) ($p < 0.05$) (Fig. 5).

Results with ZFP36L1 knockdown HCT-8 cells showed that ZFP36L1 knockdown significantly enhanced virus titer ($p < 0.05$) (Fig. 5). Knocking down ZFP36L1 facilitated the infectious virus production as early as 48 h p.i. while wild-type cells produced infectious

HCT-8 cells Viability after ZFP36L1 Overexpression or Knockdown

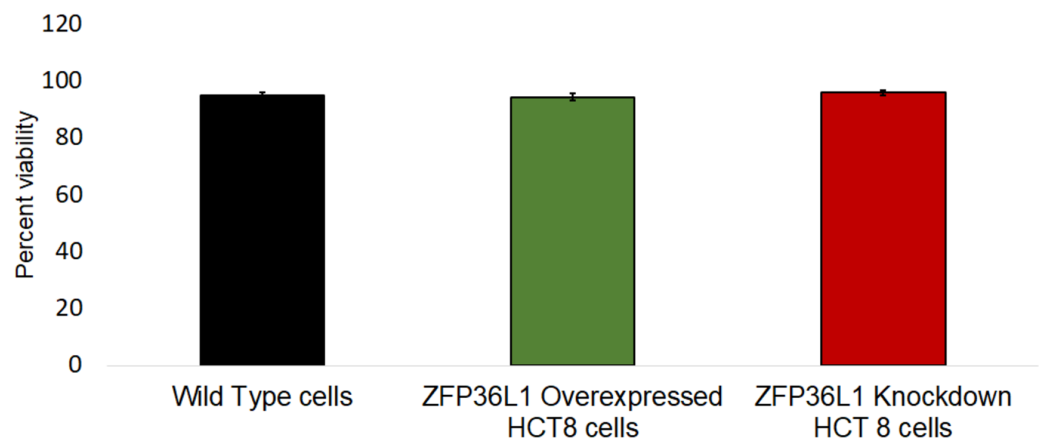


Figure 4 Effect of ZFP36L1 on HCT-8 cells viability. The effect of ZFP36L1 overexpression and its knockdown on cell viability was measured by trypan blue exclusion assay. Wild type, ZFP36L1 overexpressed and ZFP36L1 knockdown cells were individually seeded in six well plates. After 96 h post-seeding, cells were detached and stained with 0.4% trypan blue to determine the percent viability. Changes in cell viability following ZFP36L1 overexpression or its knockdown compared to wild-type cells was estimated by paired *T*-test.

Full-size DOI: 10.7717/peerj.14776/fig-4

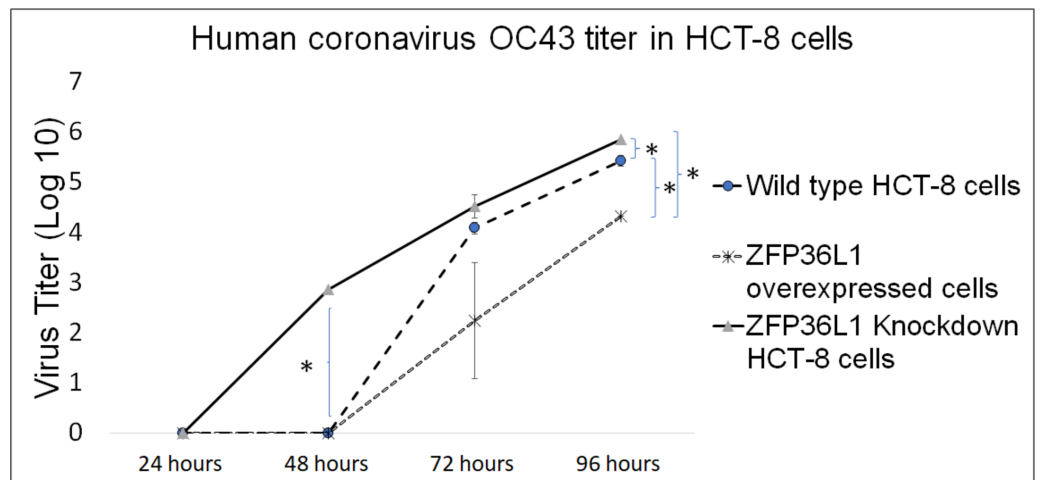


Figure 5 Human coronavirus-OC43 titer in HCT-8 cells. Wild type, ZFP36L1 overexpressed and ZFP36L1 knockdown HCT-8 cells were infected individually with HCoV-OC43 with 0.1 MOI. Supernatant from these cells was collected at 24 h, 48 h, 72 h, and 96 h p.i. and analyzed for virus titer. Asterisks show significant differences in virus titer.

Full-size DOI: 10.7717/peerj.14776/fig-5

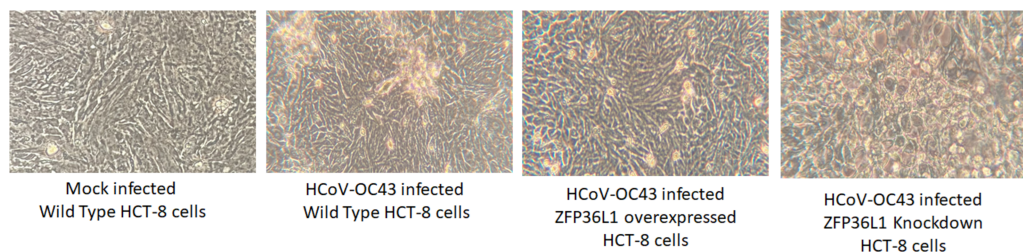


Figure 6 Effect of ZFP36L1 expression on Human coronavirus-OC43 induced cytopathic effect in HCT-8 cells. Wild type, ZFP36L1 overexpressed and ZFP36L1 knockdown HCT-8 cells were infected individually with HCoV-OC43 with 0.1 MOI. Cytopathic effect was observed at 72 h p.i. at 40 × magnification.

Full-size DOI: [10.7717/peerj.14776/fig-6](https://doi.org/10.7717/peerj.14776/fig-6)

viruses at 72 h p.i. The virus titer in ZFP36L1 knockdown cells was recorded as 00.00 ± 0.00 log 10/ml, 2.86 ± 0.00 log 10/ml, 4.52 ± 0.22 log 10/ml, and 5.85 ± 0.01 log 10/ml at 24 h, 48 h, 72 h and 96 h p.i., respectively. While wild-type HCT-8 cells have virus titer of 0.00 ± 0.00 log 10/ml, 0.00 ± 0.00 log 10/ml, 4.08 ± 0.11 log 10/ml, and 5.42 ± 0.10 log 10/ml at 24 h, 48 h, 72 h and 96 h p.i., respectively. Virus titer in ZFP36L1 knockdown cells was significantly higher at 48 h and 96 h p.i. compared to wild-type cells ($p < 0.05$) (Fig. 5). Results also showed a lower cytopathic effect in ZFP36L1 overexpressed or wild-type HCT-8 cells compared to ZFP36L1 knockdown cells at 72 h p.i. (Fig. 6)

ZFP36L1 overexpression significantly suppressed while ZFP36L1 knockdown significantly enhanced the HCoV-OC43 RNA replication

To further confirm ZFP36L1's effect on HCoV-OC43 RNA replication, wild type, ZFP36L1 overexpressed and ZFP36L1 knockdown HCT-8 cells were individually infected with HCoV-OC43 (MOI: 0.1). Infected cells were collected at 72 and 96 h p.i. Viral RNA was isolated from infected cells and viral nucleocapsid transcription (RNA concentration) was analyzed using qPCR. Results showed a significant increase in HCoV-OC43 nucleocapsid expression at 72 h and 96 h p.i. in ZFP36L1 knockdown HCT-8 cells while ZFP36L1 overexpression significantly suppressed HCoV-OC43 nucleocapsid expression at both of these time points (e.g., 72 and 96 h p.i.) ($p < 0.05$). ZFP36L1 knockdown HCT-8 cells displayed a 3.56 ± 0.77 and 7.67 ± 1.69 -fold increase in HCoV-OC43 nucleocapsid expression as compared to wild-type HCT-8 cells at 72 h and 96 h p.i., respectively (Fig. 7). ZFP36L1 overexpressed cells displayed a significantly lower HCoV-OC43 nucleocapsid expression such as 0.38 ± 0.16 and 0.16 ± 0.03 fold compared to wild-type cells at 96 h p.i. ($p < 0.05$) (Fig. 7).

DISCUSSION

The current study was designed to determine the role of ZFP36L1 (a CCCH type ZFP) on HCoV-OC43 replication. Our results showed that overexpression of ZFP36L1 significantly reduced infectious HCoV-OC43 production while ZFP36L1 knockdown significantly enhanced virus titer compared to wild-type cells. ZFP36L1 overexpression also reduced the

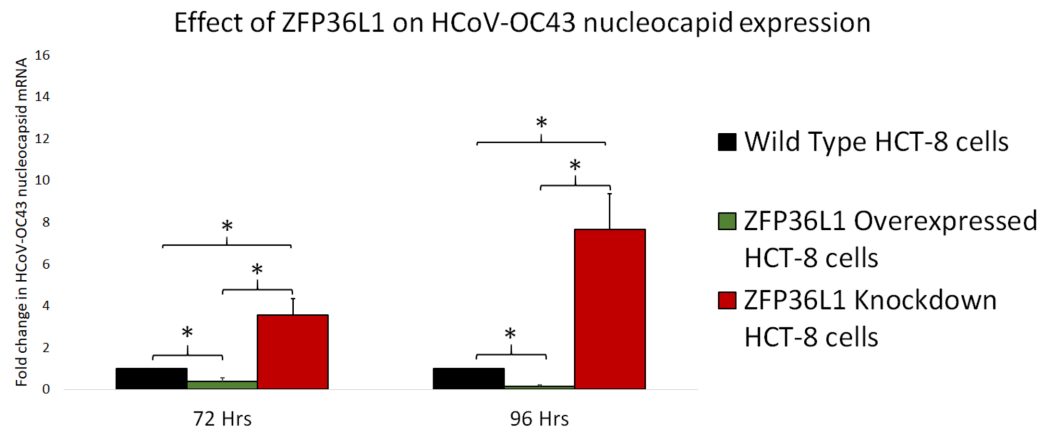


Figure 7 Effect of ZFP36L1 expression on Human coronavirus-OC43 replication. Wild-type, ZFP36L1 overexpressed and ZFP36L1 knockdown HCT-8 cells were infected individually with HCoV-OC43 with 0.1 MOI. Viral RNA was isolated from infected cells at 72 and 96 h p.i. Isolated RNA was quantified using qPCR (for viral nucleocapsid). Fold change in nucleocapsid RNA in ZFP36L1 overexpressed and knockdown cells as compared to wild-type HCT-8 cells were estimated using paired *T*-test. Asterisks show significant differences in viral RNA.

Full-size DOI: [10.7717/peerj.14776/fig-7](https://doi.org/10.7717/peerj.14776/fig-7)

RNA replication of HCoV-OC43 and suppressed the apparent cytopathic effect in infected cells.

ZFPs are one of the most abundant proteins in humans which can make up to 5% of total human proteins (Vilas *et al.*, 2018). ZFPs have an extremely high binding ability. They can bind to cellular DNA, RNA, lipids, proteins, and PAR (poly-ADP-ribose); therefore, ZFPs can modulate several cellular types of machinery (Müller *et al.*, 2007; Cassandri *et al.*, 2017; Takata *et al.*, 2017; Tang, Wang & Gao, 2017; Vilas *et al.*, 2018; Meagher *et al.*, 2019; Lal, Ullah & Syed, 2020). The diverse binding properties of ZFPs make it difficult to characterize their functional effect in cells (Vilas *et al.*, 2018). However, such a challenge is overcome by classifying the ZFPs and then identifying their functional characteristics (Cassandri *et al.*, 2017). Classification of ZFP is based on zinc ion, zinc ion interaction with specific amino acids, and the protein's folded structure (Krishna, Majumdar & Grishin, 2003). Based on such classification, CCCH-type ZFP is characterized to interact with RNA and thus modulate RNA metabolism in the cell (Maeda & Akira, 2017) including interfering with RNA virus replication (Gao, Guo & Goff, 2002; Cassandri *et al.*, 2017).

The known mechanisms by which CCCH-type ZFPs exhibit these antiviral or immunomodulatory activities is by limiting the total mRNA turnover in the cell. CCCH-type ZFPs such as ZFP36L1 have two tandem zinc finger (TZF) domains that are known to bind with adenylyl and uracyl nucleotides-rich (AU-rich) elements (AREs) in mRNA. This interaction facilitates RNA degradation by CCR4-NOT complex-mediated deadenylation, followed by 5' decapping and exonuclease-mediated nucleotide cleaving (Blackshear, 2002; Lai, Kennington & Blackshear, 2003; Lykke-Andersen & Wagner, 2005; Suk *et al.*, 2018; Lai *et al.*, 2019; Lai *et al.*, 2000).

Coronavirus genome, including HCoV-OC43's genome is 5'-capped with a 3' poly(A) tail of variable length (Fehr & Perlman, 2015). The length of the poly (A) tail varies at different

stages of the virus replication cycle and viruses with longer poly (A) tails replicate at a faster rate (Wu *et al.*, 2013). Therefore, the effect of ZFP36L1 on viral poly (A) may explain reduced virus production with ZFP36L1 overexpression in the current study. Our study not only showed that ZFP36L1 suppressed the infectious HCoV-OC43 production, but also reduced HCoV-OC43 nucleocapsid transcription indicating that ZFP36L1 mediates its antiviral effect by limiting the viral RNA in infected cells.

However, there is the possibility that ZFP36L1 can reduce virus replication with different mechanisms other than poly A tail interaction. A study showed that CCCH Type ZFP also targets the non-ARE sequence of 3' and 5' (untranslated region) UTR in mRNA (Li *et al.*, 2015). Another study showed that CCCH Type ZFP targets CG-rich viral sequences (Meagher *et al.*, 2019). The study also showed that ZFP36 (ZFP36L1) suppressed the virus production (influenza A virus) by interfering with viral protein translation/export from the nucleus to the cytoplasm without affecting viral RNA replication (Lin *et al.*, 2020). Therefore, a detailed study to determine ZFP36L1's mechanism of action for suppressing coronavirus replication needs to be explored.

CONCLUSIONS

The current study showed that overexpression of ZFP36L1, a CCCH type ZFP significantly reduced HCoV-OC43 RNA (nucleocapsid) and infectious virus production. A reduced viral production was in correlation with reduced cytopathic effect in the infected cells. Furthermore, ZFP36L1 knockdown significantly enhanced the HCoV-OC43 replication and infectious virus production. However, additional mechanisms employed to reduce virus replication still need to be explored.

ADDITIONAL INFORMATION AND DECLARATIONS

Funding

This work didn't receive any external funding.

Competing Interests

The authors declare there are no competing interests.

Author Contributions

- Tooba Momin performed the experiments, prepared figures and/or tables, authored or reviewed drafts of the article, and approved the final draft.
- Andrew Villasenor performed the experiments, prepared figures and/or tables, authored or reviewed drafts of the article, and approved the final draft.
- Amit Singh conceived and designed the experiments, analyzed the data, authored or reviewed drafts of the article, and approved the final draft.
- Mahmoud Darweesh conceived and designed the experiments, analyzed the data, authored or reviewed drafts of the article, and approved the final draft.
- Aditi Singh performed the experiments, analyzed the data, authored or reviewed drafts of the article, and approved the final draft.

- Mrigendra Rajput conceived and designed the experiments, performed the experiments, analyzed the data, prepared figures and/or tables, authored or reviewed drafts of the article, and approved the final draft.

Data Availability

The following information was supplied regarding data availability:

The raw data is available in the [Supplementary File](#).

Supplemental Information

Supplemental information for this article can be found online at <http://dx.doi.org/10.7717/peerj.14776#supplemental-information>.

REFERENCES

- Abbehausen C.** 2019. Zinc finger domains as therapeutic targets for metal-based compounds - an update. *Metallomics* **11**(1):15–28 DOI [10.1039/C8MT00262B](https://doi.org/10.1039/C8MT00262B).
- Al-Khannaq MN, Ng KT, Oong XY, Pang YK, Takebe Y, Chook JB, Hanafi NS, Kamarulzaman A, Tee KK.** 2016. Molecular epidemiology and evolutionary histories of human coronavirus OC43 and HKU1 among patients with upper respiratory tract infections in Kuala Lumpur, Malaysia. *Virology Journal* **25**(13):33 DOI [10.1186/s12985-016-0488-4](https://doi.org/10.1186/s12985-016-0488-4).
- Angiolilli C, Leijten EFA, Bekker CPJ, Eeftink E, Giovannone B, Nordkamp MO, van der Wal M, Thijs JL, Vastert SJ, van Wijk F, Radstake TRDJ, van Loosdregt J.** 2021. ZFP36 family members regulate the pro-inflammatory features of psoriatic dermal fibroblasts. *Journal of Investigative Dermatology* **142**(2):402–413.
- Bick MJ, Carroll JW, Gao G, Goff SP, Rice CM, MacDonald MR.** 2003. Expression of the zinc-finger antiviral protein inhibits alphavirus replication. *Journal of Virology* **77**(21):11555–11562 DOI [10.1128/jvi.77.21.11555-11562.2003](https://doi.org/10.1128/jvi.77.21.11555-11562.2003).
- Blackshear PJ.** 2002. Tristetraprolin and other CCCH tandem zinc-finger proteins in the regulation of mRNA turnover. *Biochemical Society Transactions* **30**(6):945–952 DOI [10.1042/bst0300945](https://doi.org/10.1042/bst0300945).
- Cassandri M, Smirnov A, Novelli F, Pitolli C, Agostini M, Malewicz M, Melino G, Raschella G.** 2017. Zinc-finger proteins in health and disease. *Cell Death Discovery* **13**(3):17071 DOI [10.1038/cddiscovery.2017.71](https://doi.org/10.1038/cddiscovery.2017.71).
- Chen SC, Jeng KS, Lai MMC.** 2017. Zinc finger-containing cellular transcription corepressor ZBTB25 promotes influenza virus RNA transcription and is a target for zinc ejector drugs. *Journal of Virology* **91**:20.
- Chen XF, Wu J, Zhang YD, Zhang CX, Chen XT, Sun JH, Chen TX.** 2018. Role of Zc3h12a in enhanced IL-6 production by newborn mononuclear cells in response to lipopolysaccharide. *Pediatrics & Neonatology* **59**(3):288–295 DOI [10.1016/j.pedneo.2017.09.006](https://doi.org/10.1016/j.pedneo.2017.09.006).
- Fehr AR, Perlman S.** 2015. Coronaviruses: an overview of their replication and pathogenesis. *Methods in Molecular Biology* **1282**:1–23 DOI [10.1007/978-1-4939-2438-7_1](https://doi.org/10.1007/978-1-4939-2438-7_1).

- Fu M, Blackshear PJ. 2017.** RNA-binding proteins in immune regulation: a focus on CCCH zinc finger proteins. *Nature Reviews Immunology* 17(2):130–143 DOI 10.1038/nri.2016.129.
- Gao G, Guo X, Goff SP. 2002.** Inhibition of retroviral RNA production by ZAP, a CCCH-type zinc finger protein. *Science* 297(5587):1703–1706 DOI 10.1126/science.1074276.
- Guo X, Carroll JW, Macdonald MR, Goff SP, Gao G. 2004.** The zinc finger antiviral protein directly binds to specific viral mRNAs through the CCCH zinc finger motifs. *Journal of Virology* 78(23):12781–12787 DOI 10.1128/JVI.78.23.12781-12787.2004.
- Hajikhezri Z, Darweesh M, Akusjärvi G, Punga T. 2020.** Role of CCCH-type zinc finger proteins in human adenovirus infections. *Viruses*. 18 12(11):1322 DOI 10.3390/v12111322.
- Haneklaus M, O’Neil JD, Clark AR, Masters SL, O’Neill LAJ. 2017.** The RNA-binding protein tristetraprolin (TTP) is a critical negative regulator of the NLRP3 inflammasome. *Journal of Biological Chemistry*. 28; 292(17):6869–6881 DOI 10.1074/jbc.M116.772947.
- Kontoyiannis DL. 2018.** An RNA checkpoint that keeps immunological memory at bay. *Nature Immunology* 19(8):795–797 DOI 10.1038/s41590-018-0168-1.
- Krishna SS, Majumdar I, Grishin NV. 2003.** Structural classification of zinc fingers: survey and summary. *Nucleic Acids Research* 31(2):532–550 DOI 10.1093/nar/gkg161.
- Lai WS, Kennington EA, Blackshear PJ. 2003.** Tristetraprolin and its family members can promote the cell-free deadenylation of AU-rich element-containing mRNAs by poly(A) ribonuclease. *Molecular and Cellular Biology* 23(11):3798–3812 DOI 10.1128/MCB.23.11.3798-3812.2003.
- Lai WS, Carballo E, Thorn JM, Kennington EA, Blackshear PJ. 2000.** Interactions of CCCH zinc finger proteins with mRNA, Binding of tristetraprolin-related zinc finger proteins to Au-rich elements and destabilization of mRNA. *Journal of Biological Chemistry* 9; 275(23):17827–17837 DOI 10.1074/jbc.M001696200.
- Lai WS, Stumpo DJ, Wells ML, Gruzdev A, Hicks SN, Nicholson CO, Yang Z, Faccio R, Webster MW, Passmore LA, Blackshear PJ. 2019.** Importance of the conserved carboxyl-terminal CNOT1 binding domain to tristetraprolin activity *in vivo*. *Molecular and Cellular Biology* 39(13):e00029-e00019 DOI 10.1128/MCB.00029-19.
- Lal S, Ullah BA, Syed S. 2020.** The role of zinc-finger antiviral proteins in immunity against viruses. *Molecular Genetics, Microbiology and Virology* 35(2):78–84 DOI 10.3103/S0891416820020020.
- Li M, Yan K, Wei L, Yang J, Lu C, Xiong F, Zheng C, Xu W. 2015.** Zinc finger antiviral protein inhibits coxsackievirus B3 virus replication and protects against viral myocarditis. *Antiviral Research* 123:50–61 DOI 10.1016/j.antiviral.2015.09.001.
- Lin RJ, Huang CH, Liu PC, Lin IC, Huang YL, Chen AY, Chiu HP, Shih SR, Lin LH, Lien SP, Yen LC, Liao CL. 2020.** Zinc finger protein ZFP36L1 inhibits influenza A virus through translational repression by targeting HA, M and NS RNA transcripts. *Nucleic Acids Research*. 27; 48(13):7371–7384 DOI 10.1093/nar/gkaa458.

- Lv L, Qin T, Huang Q, Jiang H, Chen F, Long F, Ren L, Liu J, Xie Y, Zeng M. 2021. Targeting tristetraprolin expression or functional activity regulates inflammatory response induced by MSU crystals. *Frontiers in Immunology* 16; 12:675534 DOI 10.3389/fimmu.2021.675534.
- Lykke-Andersen J, Wagner E. 2005. Recruitment and activation of mRNA decay enzymes by two ARE-mediated decay activation domains in the proteins TTP and BRF-1. *Genes & Development* 19(3):351–361 DOI 10.1101/gad.1282305.
- Maeda K, Akira S. 2017. Regulation of mRNA stability by CCCH-type zinc-finger proteins in immune cells. *International Immunology* 29(4):149–155 DOI 10.1093/intimm/dxx015.
- Matsushita K, Takeuchi O, Standley DM, Kumagai Y, Kawagoe T, Miyake T, Satoh T, Kato H, Tsujimura T, Nakamura H, Akira S. 2009. Zc3h12a is an RNase essential for controlling immune responses by regulating mRNA decay. *Nature*. 30; 458(7242):1185–1190 DOI 10.1038/nature07924.
- Meagher J, Takata M, Gonçalves-Carneiro D, Keane SC, Rebendenne A, Ong H, Orr VK, MacDonald MR, Stuckey JA, Bieniasz PD, Smith JL. 2019. Structure of the zinc-finger antiviral protein in complex with RNA reveals a mechanism for selective targeting of CG-rich viral sequences. *Proceedings of the National Academy of Sciences of the United States of America* 116(48):24303–24309 DOI 10.1073/pnas.1913232116.
- Mino T, Murakawa Y, Fukao A, Vandenbon A, Wessels HH, Ori D, Uehata T, Tartey S, Akira S, Suzuki Y, Vinuesa CG, Ohler U, Standley DM, Landthaler M, Fujiwara T, Takeuchi O. 2015. Regnase-1 and roquin regulate a common element in inflammatory mRNAs by spatiotemporally distinct mechanisms. *Cell*. 21; 161(5):1058–1073 DOI 10.1016/j.cell.2015.04.029.
- Müller S, Möller P, Bick MJ, Wurr S, Becker S, Günther S, Kümmerer BM. 2007. Inhibition of filovirus replication by the zinc finger antiviral protein. *Journal of Virology* 81(5):2391–2400 DOI 10.1128/JVI.01601-06.
- Musah RA. 2004. The HIV-1 nucleocapsid zinc finger protein as a target of antiretroviral therapy. *Current Topics in Medicinal Chemistry* 4(15):1605–1622 DOI 10.2174/1568026043387331.
- Reed LJ, Muench J. 1938. A simple method of estimating fifty percent endpoints. *American Journal of Epidemiology* 27(3):493–497 DOI 10.1093/oxfordjournals.aje.a118408.
- Schito ML, Soloff AC, Slovitz D, Trichel A, Inman JK, Appella E, Turpin JA, Barratt-Boyes SM. 2006. Preclinical evaluation of a zinc finger inhibitor targeting lentivirus nucleocapsid protein in SIV-infected monkeys. *Current HIV Research* 4(3):379–386 DOI 10.2174/15701620677709492.
- Schneider C, Rasband W, Eliceiri K. 2012. NIH Image to ImageJ: 25 years of image analysis. *Nature Methods* 9:671–675 DOI 10.1038/nmeth.2089.
- Scozzafava A, Owa T, Mastrolorenzo A, Supuran CT. 2003. Anticancer and antiviral sulfonamides. *Current Medicinal Chemistry* 10(11):925–953 DOI 10.2174/0929867033457647.
- Shrestha A, Pun NT, Park PH. 2018. ZFP36L1 and AUF1 induction contribute to the suppression of inflammatory mediators expression by globular adiponectin via

- autophagy induction in macrophages. *Biomolecules & Therapeutics* **26**(5):446–457 DOI [10.4062/biomolther.2018.078](https://doi.org/10.4062/biomolther.2018.078).
- Strober W.** 2015. Trypan blue exclusion test of cell viability. *Current Protocols in Immunology* **2**(111):A3.B.1–A3.B.3 DOI [10.1002/0471142735.ima03bs111](https://doi.org/10.1002/0471142735.ima03bs111).
- Stumpo DJ, Lai WS, Blackshear PJ.** 2010. Inflammation: cytokines and RNA-based regulation. *Wiley Interdisciplinary Reviews:RNA* **1**(1):60–80 DOI [10.1002/wrna.1](https://doi.org/10.1002/wrna.1).
- Suk FM, Chang CC, Lin RJ, Lin SY, Liu SC, Jau CF, Liang YC.** 2018. ZFP36L1 and ZFP36L2 inhibit cell proliferation in a cyclin D-dependent and p53-independent manner. *Scientific Reports* **9**(8(1)):2742 DOI [10.1038/s41598-018-21160-z](https://doi.org/10.1038/s41598-018-21160-z).
- Takata MA, Gonçalves-Carneiro D, Zang TM, Soll SJ, York A, Blanco-Melo D, Bieniasz PD.** 2017. CG dinucleotide suppression enables antiviral defence targeting non-self RNA. *Nature* **550**(7674):124–127 DOI [10.1038/nature24039](https://doi.org/10.1038/nature24039).
- Tu Y, Wu X, Yu F, Dang J, Wang J, Wei Y, Cai Z, Zhou Z, Liao W, Li L, Zhang Y.** 2019. Tristetraprolin specifically regulates the expression and alternative splicing of immune response genes in HeLa cells. *BMC Immunology*, **20**(1):13 DOI [10.1186/s12865-019-0292-1](https://doi.org/10.1186/s12865-019-0292-1).
- Tang Q, Wang X, Gao G.** 2017. The short form of the zinc finger antiviral protein inhibits influenza A virus protein expression and is antagonized by the virus-encoded NS1. *Journal of Virology* **91**(2):e01909–e01916.
- Uehata T, Akira S.** 1829. 2013. mRNA degradation by the endoribonuclease Regnase-1/ZC3H12a/MCPIP-1. *Biochimica et Biophysica Acta* **1829**(6-7):708–713.
- Vilas CK, Emery LE, Denchi EL, Miller KM.** 2018. Caught with One's Zinc fingers in the genome integrity cookie jar. *Trends in Genetics* **34**(4):313–325 DOI [10.1016/j.tig.2017.12.011](https://doi.org/10.1016/j.tig.2017.12.011).
- Wang KT, Wang HH, Wu YY, Su YL, Chiang PY, Lin NY, Wang SC, Chang GD, Chang CJ.** 2015. Functional regulation of Zfp36l1 and Zfp36l2 in response to lipopolysaccharide in mouse RAW264.7 macrophages. *Journal of Inflammation* **16**(12):42 DOI [10.1186/s12950-015-0088-x](https://doi.org/10.1186/s12950-015-0088-x).
- Wawro M, Kochan J, Kasza A.** 2016. The perplexities of the ZC3H12A self-mRNA regulation. *Acta Biochimica Polonica* **63**(3):411–415.
- Wu HY, Ke TY, Liao WY, Chang NY.** 2013. Regulation of coronaviral poly(A) tail length during infection. *PLOS ONE* **29**(8(7)):e70548 DOI [10.1371/journal.pone.0070548](https://doi.org/10.1371/journal.pone.0070548).
- Zhang B, Goraya MU, Chen N, Xu L, Hong Y, Zhu M, Chen JL.** 2020. Zinc finger CCCH-type antiviral protein 1 restricts the viral replication by positively regulating type I interferon response. *Frontiers in Microbiology* **11**:1912–1912 DOI [10.3389/fmicb.2020.01912](https://doi.org/10.3389/fmicb.2020.01912).
- Zhao Y, Song Z, Bai J, Liu X, Nauwynck H, Jiang P.** 2019. ZAP, a CCCH-type zinc finger protein, inhibits porcine reproductive and respiratory syndrome virus replication and interacts with Viral Nsp9. *Journal of Virology* **93**(10):e00001-19 DOI [10.1128/JVI.00001-19](https://doi.org/10.1128/JVI.00001-19).
- Zhu M, Ma X, Cui X, Zhou J, Li C, Huang L, Shang Y, Cheng Z.** 2017. Inhibition of avian tumor virus replication by CCCH-type zinc finger antiviral protein. *Oncotarget*. **19**; **8**(35):58865–58871 DOI [10.18632/oncotarget.19378](https://doi.org/10.18632/oncotarget.19378).

- Zhu M, Zhou J, Liang Y, Nair V, Yao Y, Cheng Z. 2020.** CCCH-type zinc finger antiviral protein mediates antiviral immune response by activating T cells. *Journal of Leukocyte Biology* **107**(2):299–307 DOI [10.1002/JLB.1AB1119-314RRR](https://doi.org/10.1002/JLB.1AB1119-314RRR).
- Zhu Y, Chen G, Lv F, Wang X, Ji X, Xu Y, Sun J, Wu L, Zheng YT, Gao G. 2011.** Zinc-finger antiviral protein inhibits HIV-1 infection by selectively targeting multiply spliced viral mRNAs for degradation. *Proceedings of the National Academy of Sciences of the United States of America*. *20*; **108**(38):15834–15839 DOI [10.1073/pnas.1101676108](https://doi.org/10.1073/pnas.1101676108).